LJMU Research Online

Kelley, NP, Irmis, RB, DePolo, PE, Noble, PJ, Montague-Judd, D, Little, H, Blundell, J, Rasmussen, C, Percival, LME, Mather, TA and Pyenson, ND

 Grouping behavior in a Triassic marine apex predator

http://researchonline.ljmu.ac.uk/id/eprint/25362/

Article

For more information please contact researchonline@ljmu.ac.uk

Current Biology

Grouping behavior in a Triassic marine apex predator

Highlights

- Abundant fossils from Nevada reflect aggregations of a predatory marine reptile

- Nearly all individuals are large adults apart from multiple embryos or neonates

- No evidence for significant environmental perturbation is found

Authors

Neil P. Kelley, Randall B. Irmis, Paige E. dePolo, ..., Lawrence M.E. Percival, Tamsin A. Mather, Nicholas D. Pyenson

Correspondence

neil.p.kelley@vanderbilt.edu

In brief

Kelley et al. provide an extensive reappraisal of an unsual Triassic marine reptile fossil assemblage using site-scale 3D digitization and other techniques and present data for grouping behavior in an extinct marine predator.

CelPress

Report

Grouping behavior in a Triassic marine apex predator

Neil P. Kelley,[1,11,12,*] Randall B. Irmis,[2,3] Paige E. dePolo,[4,5] Paula J. Noble,[5] Danielle Montague-Judd,[2,6] Holly Little,[1] Jon Blundell,[7] Cornelia Rasmussen,[2,8] Lawrence M.E. Percival,[9,10] Tamsin A. Mather,[10] and Nicholas D. Pyenson[1]

[1]Department of Paleobiology, National Museum of Natural History, Smithsonian Institution, 1001 Madison Drive NW, Washington, DC 20560, USA
[2]Natural History Museum of Utah, University of Utah, 301 Wakara Way, Salt Lake City, UT 84108, USA
[3]Department of Geology & Geophysics, University of Utah, 115 S 1460 E, Salt Lake City, UT 84112, USA
[4]School of GeoSciences, University of Edinburgh, Grant Institute, James Hutton Road, Edinburgh, Scotland EH9 3FE, UK
[5]Department of Geological Sciences and Engineering, University of Nevada—Reno, 1664 N. Virginia Street, Reno, NV 89557, USA
[6]Department of Geosciences, University of Arizona, 1040 E 4th St, Tucson, AZ 85721, USA
[7]Digitization Program Office 3D Lab, Office of the Chief Information Officer, Smithsonian Institution, Landover, MD 20758, USA
[8]Institute for Geophysics, Jackson School of Geosciences, University of Texas at Austin, 2305 Speedway Stop C1160, Austin, TX 78712-1692, USA
[9]Analytical, Environmental and Geochemistry Group (AMGC), Vrije Universiteit Brussel, Pleinlaan 2, Brussels 1050, Belgium
[10]Department of Earth Sciences, University of Oxford, South Parks Road, Oxford OX1 3AN, UK
[11]Present address: Department of Earth and Environmental Sciences, Vanderbilt University, PMB 351805 2301 Vanderbilt Place, Nashville, TN 37235-1805, USA
[12]Lead contact
*Correspondence: neil.p.kelley@vanderbilt.edu
https://doi.org/10.1016/j.cub.2022.11.005

SUMMARY

Marine tetrapods occupy important roles in modern marine ecosystems and often gather in large aggregations driven by patchy prey distribution,[1,2] social or reproductive behaviors,[3,4] or oceanographic factors.[5] Here, we show that similar grouping behaviors evolved in an early marine tetrapod lineage, documented by dozens of specimens of the giant ichthyosaur *Shonisaurus* in the Luning Formation in West Union Canyon, Nevada, USA.[6,7] A concentration of at least seven skeletons closely preserved on a single bedding plane received the bulk of previous attention. However, many more specimens are preserved across ~10^6 square meters and ~200 stratigraphic meters of outcrop representing an estimated >10^{5-6} years. Unlike other marine-tetrapod-rich deposits, this assemblage is essentially monotaxic; other vertebrate fossils are exceptionally scarce. Large individuals are disproportionately abundant, with the exception of multiple neonatal or embryonic specimens, indicating an unusual demographic composition apparently lacking intermediate-sized juveniles or subadults. Combined with geological evidence, our data suggest that dense aggregations of *Shonisaurus* inhabited this moderately deep, low-diversity, tropical marine environment for millennia during the latest Carnian Stage of the Late Triassic Period (237–227 Ma). Thus, philopatric grouping behavior in marine tetrapods, potentially linked to reproductive activity, has an antiquity of at least 230 million years.

RESULTS AND DISCUSSION

Marine tetrapods are ecologically important members of ocean ecosystems, directly influencing nutrient cycling and ecosystem structure, in part because of their relatively large body sizes and high mobility.[8,9] Top marine predators today frequently coordinate seasonal migrations, forming transient aggregations or persistent social groups, with effects that further modulate their impacts on marine ecosystems. Understanding the significance of these ecological dynamics over geologic timescales requires fossil data.[10,11] Fossil sites with exceptional abundance and/or preservation can provide critical ecological snapshots that are otherwise unavailable. However, investigations into the genesis of exceptional marine tetrapod-bearing deposits have often focused on the physical and environmental controls on fossil accumulation and preservation.[12,13] In contrast, the insights into behavioral and ecological dynamics provided by marine tetrapod fossil assemblages have received much less attention.

The Luning Formation at Berlin-Ichthyosaur State Park (BISP) in West Union Canyon (WUC), central Nevada, USA, contains an unusual marine tetrapod assemblage preserving dozens of associated skeletons and fragmentary specimens of the Late Triassic giant ichthyosaur *Shonisaurus popularis*.[6,7] Although individuals of *Shonisaurus* have been discovered at multiple sites across ~2 km² in WUC (Figures 1 and S2), most attention since the mid 20th century has focused on a high concentration of articulated skeletons left *in situ* on a single bedding plane, called Quarry 2 (Figures 1, 2, and S1). Hypotheses ranging from stranding to mass mortality have been proposed for the skeletal concentration at Quarry 2, but none of them are well supported by geologic or taphonomic evidence.[6,7,14] Beyond Quarry 2, the broader significance of the abundance of *Shonisaurus* and the
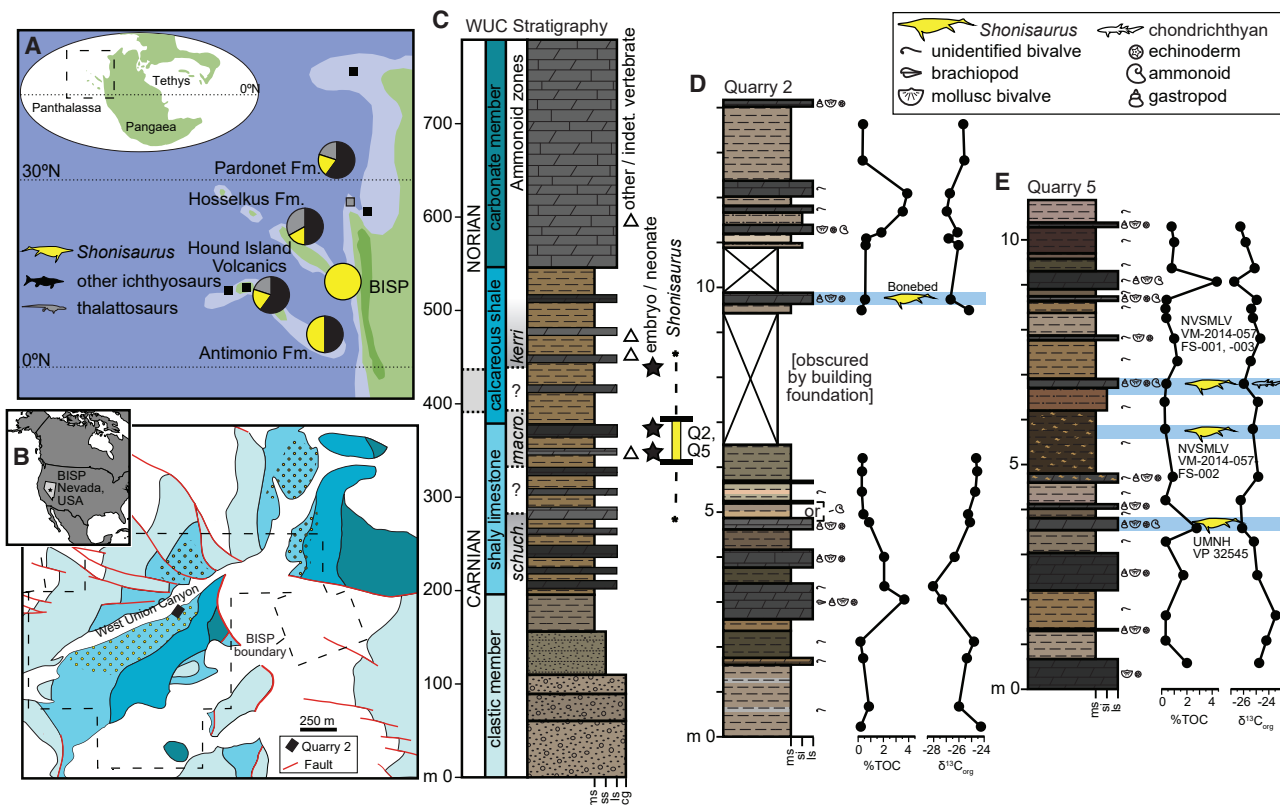
Figure 1. Geographic, geologic, and stratigraphic context of ichthyosaur occurrences at WUC

(A) Paleogeography of the Late Triassic Period adapted from Martindale et al.[15] indicating the distribution of *Shonisaurus* and other marine reptiles. Pie charts denote major assemblages, and squares mark isolated occurrences; (B) geologic map of West Union Canyon (WUC) adapted from,[14] dotted areas denote where *Shonisaurus* fossils have been found in WUC; (C) summarized stratigraphy of WUC based on Balini et al.[14] and Silberling,[16] indicating the occurrence of *Shonisaurus* and other vertebrate fossils, and stratigraphic position of Quarry 2 (Q2) and Quarry 5 (Q5) is approximate. ms, mudstone; ss, sandstone; ls, limestone; cg, conglomerate; and (D) and (E) stratigraphy and geochemistry of key sites within WUC Quarry 2 (mass mortality) and Quarry 5 (type locality), and blue bars indicate ichthyosaur-bearing horizons.

See also Figures S2–S4, Tables 1 and S2, and Methods S1.

dearth of other marine vertebrate taxa across multiple horizons within the Luning Formation at WUC remains poorly understood.

Geology, geochemistry, and taphonomy

We investigated the geology and taphonomy of previously known localities including Quarry 2 and the *Shonisaurus* type locality (Quarry 5) and surveyed the distribution of vertebrate fossils across WUC (Figure 1B). We identified and georeferenced 112 vertebrate specimens from 50 distinct localities including the *in situ* specimens in Quarry 2 (Table 1, global positioning system [GPS] coordinates of all localities on file with UMNH). *Shonisaurus* occurs at multiple horizons within two members of the Luning Formation, spanning three ammonoid zones.[16] Although specimens referable to *Shonisaurus* are present in three ammonoid zones (Figure 1C), the majority are from the latest Carnian *Klamathites macrolobatus* zone, including Quarry 5 and the bonebed at Quarry 2, clarifying a discrepancy among previous descriptions.[6,7,14] Except for a few non-diagnostic bone fragments, we identify all tetrapod occurrences as ichthyosaurian based on porous bone texture lacking an outer cortical layer.[17] Moreover, all diagnostic elements invariably showed additional features typical of *Shonisaurus*, including massive ribs with a round

cross-section, very large amphicoelous vertebral centra with a high width-to-length ratio and lacking attached neural arches, massive and distinctive limb and girdle elements, including sub-rectangular humeri and proximally expanded coracoids, and deep jaw fragments bearing large teeth with highly infolded roots set in distinct sockets (Figures 3A–3E).[6,18] Non-ichthyosaur macrovertebrate specimens are exceedingly scarce, comprising an elasmobranch fin spine, small osteichthyan bones, and indeterminate bone fragments (Table 1), consistent with what has been previously reported for the site.[6]

Fossil-bearing strata at BISP comprise organic mudstones interspersed with thinner carbonate horizons; the latter units are predominantly wackestones and packstones with abundant disarticulated bivalves, echinoids, and other invertebrates. This sedimentology is consistent across ichthyosaur-bearing horizons and suggests deposition below fair-weather wave base but above maximum storm wave base (Figure S4; Methods S1). *Shonisaurus* fossils are present in both mudstone and carbonate facies (Figure 1C). This moderately deep distal ramp setting (cf. Hogler[7]) excludes an earlier hypothesis of stranding for the ichthyosaur assemblage,[6] unless stranded carcasses were transported to deeper water *en masse*, an unlikely
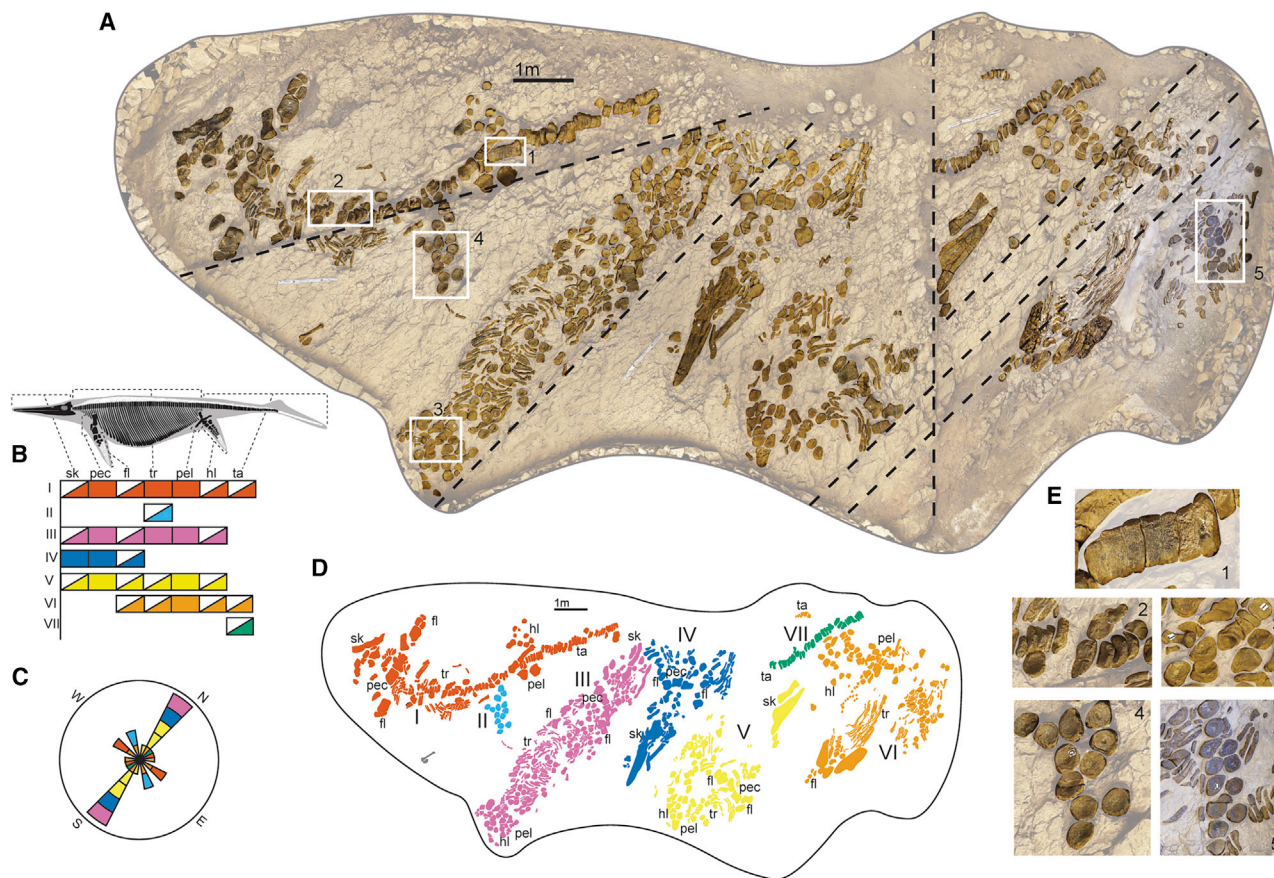
Figure 2. Taphonomic interpretation of Quarry 2

(A) Orthographic view of mass mortality layer (Quarry 2) generated by photogrammetry and laser scanning; (B) taphonomic state of quarry 2 skeletons by skeletal region, half-filled boxes <50% complete, filled boxes >50% complete, sk, skull; pec, pectoral girdle; fl, forelimb; tr, trunk; hl, hindlimb; ta, tail; (C) rose diagram indicating directional orientation of skeletal units; (D) interpretation of mass mortality layer; Roman numerals designate discrete skeletons; and (E) sequence showing successive stages of disarticulation of vertebral columns, and white rectangles on panel a indicate position of each view.
See also Figures S1 and S2 and Table S3.

hypothesis that is difficult to test. There is no direct geological evidence for a major environmental perturbation (e.g., ocean anoxia, carbon cycle changes, or volcanic eruptions) either coeval with or immediately prior/following deposition of the Quarry 2 bonebed that might provide a repeated kill mechanism. The latest Carnian *macrolobatus* zone post-dates the Carnian Pluvial Episode (CPE) by at least 2–3 million years[19] but is within known uncertainties for the eruption of the Wrangellia flood basalts (~234–225 Ma).[20] Although there is some variability above and below the bonebed in Quarry 2, the *Shonisaurus*-rich layer itself shows no evidence of a clear mercury (Hg) peak or increased enrichment with respect to total organic carbon (TOC) (i.e., increased Hg/TOC) that would imply a large subaerial eruptive event as a driver of increased ichthyosaur mortality and would result in the preserved fossil assemblage at that site (Figure S3; Methods S1). This absence of a clear peak contrasts with the more coherent signals attributed to the Wrangellia eruptions observed in more distal western Tethys successions associated with the CPE itself.[21] Similarly, *Shonisaurus*-bearing horizons in quarries 2 and 5 do not stratigraphically correlate with any observed excursions in the organic carbon isotope ($\delta^{13}C_{org}$)

record. Although negative $\delta^{13}C_{org}$ excursions can record disruption of primary productivity or a flux of isotopically light carbon to the ocean-atmosphere system,[22] the most negative values in WUC are not associated with ichthyosaur-rich horizons and nor are large-scale carbon cycle perturbations thought to have occurred during the late Carnian. Instead, the high TOC content of samples with lower $\delta^{13}C_{org}$ values suggests that they likely reflect locally increased carbon burial (Figures 1D and 1E; Figure S3; Methods S1) or a change in the aggregate composition of organic matter. Thus, we find no clear evidence for a persistent environmental mechanism biased toward killing or preserving *Shonisaurus*.

Although most occurrences of *Shonisaurus* within WUC are isolated individuals, in at least three localities (Figure S2; Table S3), multiple individuals occur in proximity sometimes on the same stratigraphic level. This is most striking at Quarry 2 where we identified twelve distinct clusters of associated or articulated bones (Figures 2A and S1; Tables 1 and S3). Some of these likely represent multiple portions of the same animal fragmented by taphonomic processes. Four partial skulls with associated pectoral girdles provide a conservative minimum number

Table 1. West Union Canyon vertebrate fossil specimens by ammonoid zone and taphonomic state

Taxon	Ammonoid zone	Taphonomic state		
		Isolated	Associated	Semi-articulated
Shonisaurus sp.	*S. kerri*	1	1	–
	K. macrolobatus	8	59	9
	K. schucherti	2	1	–
Ichthyosauria indet. (cf. *Shonisaurus* sp.)	*K. macrolobatus*	19	5	–
	K. schucherti	3	–	–
Other vertebrates				
Chondrichthyes	*K. macrolobatus*	1	–	–
Actinopterygii	*S. kerri*	1	–	–
Vertebrata indet.	*S. kerri* (or above)	2	–	–

See also Table S3 and Methods S1.

of individuals. Based on position and arrangement of clusters, we estimate that at least seven individuals are preserved in the quarry (Figure 2D), although previous estimates of nine individuals[7] cannot be conclusively rejected. Original excavations revealed as many as six additional partial skeletons near Quarry 2[6] (Figure S2); these could represent an extension of the bone bed, but the fate of most of this material is unknown, and the limited available information renders this hypothesis equivocal. Although the Quarry 2 specimens are all associated, their taphonomic condition ranges widely (Figure 2B). Most clusters within Quarry 2 exhibit a parallel alignment (Figure 2C) and are lacking smaller elements including distal limbs and tail, suggesting variably moderate-to-high degrees of decay, disarticulation, and hydraulic modification prior to burial. Petrographic analysis of the bone-bearing carbonate layer in Quarry 2 shows a dense concentration of broken invertebrate shell fragments with preferential alignment subparallel to bedding in a fine-grained carbonate mud matrix (Figure S4; Methods S1), consistent with transient elevated energy levels below fair-weather wave base and similar to the sedimentology observed at quarries 5 and 6. Differential degrees of articulation and completeness reflect varying degrees of decay prior to burial and suggest that some carcasses were either floating in the water column or sitting on the seabed for some time prior to burial.[23]

In contrast, at other WUC *Shonisaurus* sites, specimens show a wider range of taphonomic conditions. Apart from quarry 2, at least four other localities are known to preserve partially articulated skeletons including the original type locality and a newly discovered site (Figure S2; Table S3). However, isolated bones found *in situ* at multiple locations in WUC demonstrate that some skeletons were fully disarticulated prior to burial. Articulated remains appear to be more common in the *macrolobatus* zone (Table 1), which coincides with an overall maximum abundance of *Shonisaurus* occurrences, including isolated and disarticulated remains (Figure 1C). Original excavations documented fragmentary but associated or partially articulated remains in the underlying *schucherti* zone[6]; however, *Shonisaurus* fossils are

more sparsely distributed in these lower horizons, and we did not discover additional articulated remains within this interval (Figure 1C; Table 1).

Age structure

The majority of *Shonisaurus* specimens from WUC represent very large individuals spanning a narrow size class, both in Quarry 2 and at other WUC localities, based on comparisons of humerus length (a frequently used proxy for body size in ichthyosaurs[24–26]) and other skeletal proportions (Figures 3F and 3G; Table S1). Humeri within Quarry 2 range from 31 to 45 cm in length and all others known from WUC fall within this range. Based on previously published correlations between ichthyosaur humerus length and total body length, this corresponds to total estimated body lengths of WUC *Shonisaurus* ranging from 11 to 16 m, consistent with earlier estimates.[6,18,27] The restricted size distribution across WUC *Shonisaurus* specimens, limited to very large individuals, contrasts with other marine reptile lägerstatten which preserve a more complete postnatal ontogenetic sample including juveniles, subadults, and adults.[28–30]

Although the vast majority of *Shonisaurus* occurrences in WUC represent large, skeletally mature individuals, we identified three discrete occurrences representing embryonic or neonatal individuals. One specimen (NSMLV VM-2014-057-FS-001) consists of a mass of small bones from the pelvic region of the type *Shonisaurus* specimen (Figure 3H; supplemental information); it was previously noted in the original description of the taxon[6] but never figured or described in detail. Another small isolated centrum associated with the type material was identified in collections (NSMLV VM-2014-057-FS-007, Figure S5B). Our μCT analyses confirm the identification of these elements as extremely small *Shonisaurus* vertebrae, based on their high diameter to length ratio and overall similarity in shape and proportion to adult *Shonisaurus* centra (supplemental information). A very small surface-collected, isolated vertebral centrum (UMNH VP 32547, Figure S5C) found in a different area of WUC is a close match with those found *in situ* within the type specimen (supplemental information). Finally, a surface-collected fragmentary jaw (UCMP 290269) exhibits teeth with heavily plicated roots set in discrete sockets separated by thin bony partitions consistent with the distinctive dentition observed in adult *Shonisaurus popularis* (Figures 3A–3E and S5A). Thus, the size distribution of the WUC *Shonisaurus* assemblage is markedly bimodal, with large individuals and embryos/neonates, but no observed intermediately sized juveniles (Figures 3F and 3G).

Paleoecological implications

The large size of *Shonisaurus*, together with new specimens preserving robust sectorial teeth throughout the jaws (Figures 3A, 3C, 3D, and 3E), indicate a trophic role as a macrophagous raptorial predator that likely fed at least in part on large-bodied prey, i.e., the so-called "cut guild,[31]" as opposed to previous suggestions of specialized filter feeding[32] or suction feeding.[33] However, there are very few potential large prey items preserved within the Luning Formation at WUC. This scarcity does not appear to be due to preservation bias as large *Shonisaurus* and small invertebrate fossils, including ammonoids and bivalves, are very abundant at the site. We therefore propose that *Shonisaurus* likely fed elsewhere, consistent with wide ranging foraging activities of most large
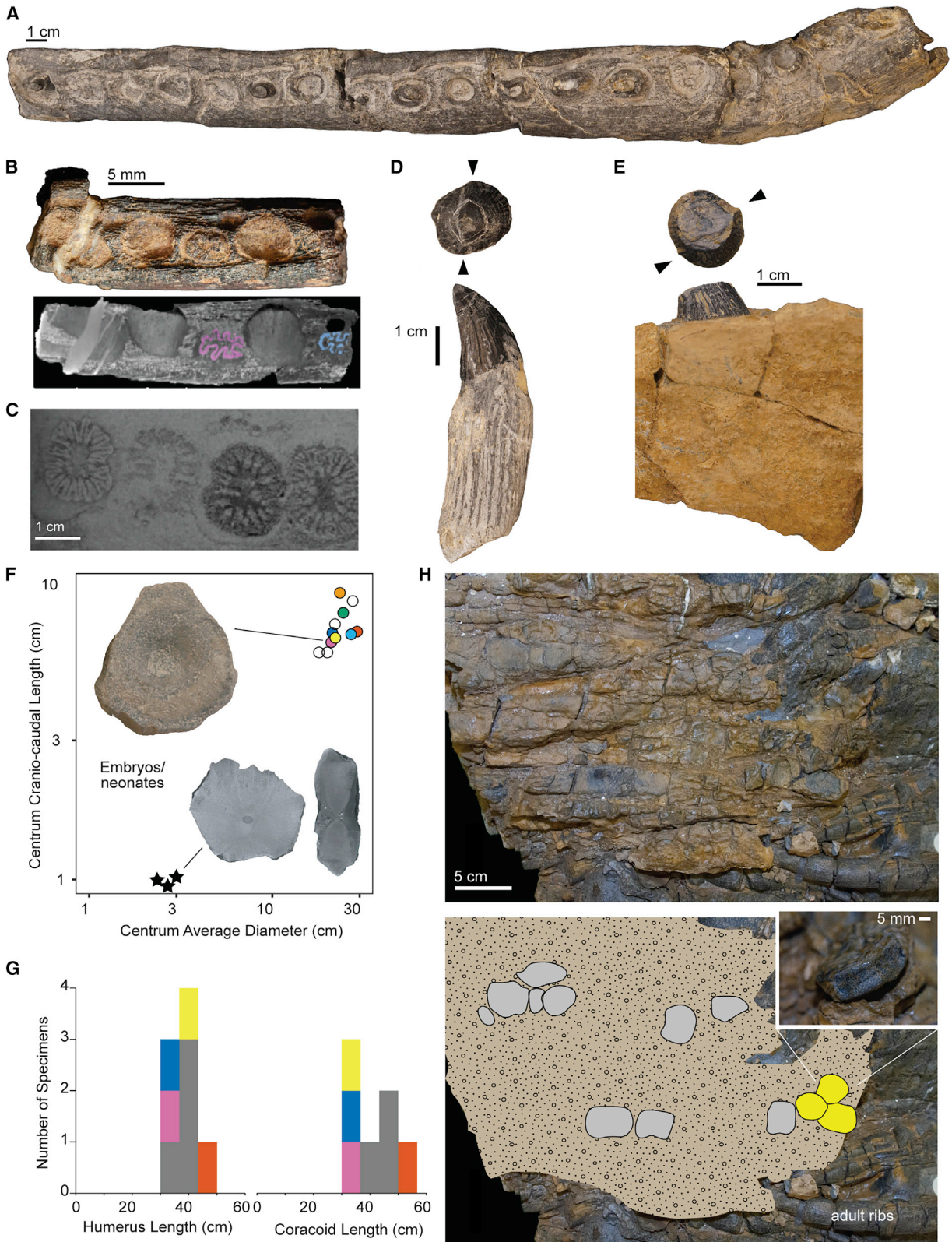
Figure 3. Select ichthyosaur fossils from WUC illustrating overall size distribution and anatomy
(A) Lower jaw (dentary) from adult *Shonisaurus* (UMNH VP 32539); (B) above: embryo or neonate jaw (UCMP 290269), below: μCT scan of same showing five alveoli and two *in situ* infolded tooth-roots; (C) μCT of adult *Shonisaurus* jaw (BISP 10); (D) complete tooth from UMNH VP 32539 showing characteristic features including deep, infolded root and carinae; (E) partial jaw (UMNH VP 32535) with *in situ* tooth missing distal tip of crown; (F) dimensions of largest vertebral centra,

(legend continued on next page)

extant marine tetrapods.[8] Indeed, *Shonisaurus* fossils are also abundant in other Luning Formation exposures about 60 km southwest of WUC in the Pilot Mountains of Nevada,[34,35] suggesting a broader regional distribution within the partially restricted seaway in which these marine sediments were deposited. Outside of the Luning Formation, specimens referred to *Shonisaurus* occur in other Late Triassic marine deposits associated with accreted arc terranes preserved in Sonora, Mexico,[36,37] southeastern Alaska,[38] and possibly northern California.[37] Despite lower sample sizes, outside of the Luning Formation, *Shonisaurus* occurs in association with other marine reptile taxa and other vertebrates and likely occupied a top-predator role in multi-tiered marine food webs (Figure 1A). The large size of *Shonisaurus* is also consistent with long distance travel, as the co-evolution of migration and body size, modulated by dynamics such as climate and patchy prey distribution, has been suggested for other marine tetrapod clades.[39]

Abundant *Shonisaurus* fossil occurrences in WUC span approximately 200 m of section and more than a complete ammonoid biozone representing $>10^{5-6}$ years[40] (Figure 1C; supplemental information). The preponderance of large individuals, the scarcity of other large marine vertebrate fossils, the presence of both *in situ* and isolated embryonic or neonatal specimens, and records of *Shonisaurus* from other approximately coeval localities spanning ~30° of paleolatitude and a range of paleoenvironments (Figure 1A) are all consistent lines of evidence with a scenario tied to reproductive aggregation and/or seasonal migration. This scenario involves sexually mature, in some cases gravid, individuals aggregating together in groups in the absence of potential predators that would target newborns. These dense aggregations would have been vulnerable to mortality events and subsequent burial penecontemporaneously, as observed at Quarry 2, although many WUC *Shonisaurus* occurrences, which range from isolated and disarticulated to nearly complete specimens at multiple stratigraphic levels, likely represent attritional mortality. Thus, although Quarry 2 is notable in preserving a large number of associated skeletons, it is representative of the larger-scale pattern of an essentially monotypic marine tetrapod assemblage of *Shonisaurus* throughout WUC.

Although the WUC assemblage is far from unique in preserving ichthyosaur embryos,[41–43] it does contrast with most other ichthyosaur-bearing lägerstatten by the absence other marine reptile taxa, even other species of ichthyosaurs, and scarcity of intermediate-sized juveniles or subadults. However, it is possible that grouping behavior linked to seasonal reproductive cycles played a role in the genesis of other ichthyosaur-rich fossil assemblages. Notably, group migratory behavior is a common feature of many extant marine tetrapods and other large marine vertebrates. For example, baleen whales seek out lower productivity water to give birth, either to avoid potential predators[44] or for energetic reasons.[45]

Conclusions

The Mesozoic Era marks a pivotal interval in the modernization of marine and terrestrial ecosystems across all trophic levels.[46,47] This transition was initiated during the Triassic, in the wake of the end-Permian mass extinction. By the Middle Triassic, 5 million years later, ichthyosaurs evolved the large body sizes typical of dominant predators at the top of marine food webs.[48,49] This role has been occupied by successive lineages of marine tetrapod predators ever since, punctuated by turnovers driven by extinctions and radiations of new marine clades.[50] Triassic ichthyosaurs were among the first marine tetrapods to acquire key innovations, such as high-performance swimming,[51] deep diving,[52,53] and aquatic birth,[41] many of which evolved convergently among other Mesozoic marine reptiles and over 130 million years later in seabirds and marine mammals.

The results presented here underscore an additional behavioral trait that emerged early in ichthyosaur evolution: grouping behavior of adults. The ichthyosaur aggregations recorded in the Luning Formation at WUC seem to have occurred in the absence of an abundant prey source, suggesting that *Shonisaurus* might have regularly traveled between birthing and feeding grounds. Similar mass movements are observed in the life history of many marine tetrapods today, including whales,[54] pinnipeds,[3] and penguins.[4] Grouping behaviors of large marine predators amplify their impacts on ecosystems and their long-distance movements link spatio-temporally distinct habitats. Our results suggest that marine tetrapods have participated in these dynamics for more than 230 million years.

STAR★METHODS

Detailed methods are provided in the online version of this paper and include the following:

- KEY RESOURCES TABLE
- RESOURCE AVAILABILITY
  - Lead contact
  - Materials availability
  - Data and code availability
- EXPERIMENTAL MODEL AND SUBJECT DETAILS
  - Museum abbreviations
  - Information about the specimens
- METHOD DETAILS
  - Capturing, processing and rendering 3D digital datasets
  - Taphonomy and size distribution
  - Field investigation and geological methods
- QUANTIFICATION AND STATISTICAL ANALYSIS

SUPPLEMENTAL INFORMATION

Supplemental information can be found online at https://doi.org/10.1016/j.cub.2022.11.005.

and colored specimens indicate Quarry 2 specimens (vertebrae shown is from BISP Quarry 2 specimen III) starred specimens embryo or neonatal material (NSM-LV VM-2014-057-FS-001 shown); (G) comparison of humerus and coracoid lengths, and colored specimens are Quarry 2 specimens following colors of Figure 2; (H) above: *in situ* embryo vertebrae within posterior rib block of *Shonisaurus* holotype (NSM-LV VM-2014-057-FS-001), below: interpretive line drawing of *in situ* embryo remains, yellow bones were removed for μCT scanning (shown in F and supplemental information), gray bones have not yet been prepared or scanned, and brown stippled regions shows area partially covered by matrix.

See also Figure S4, Table S1, and Methods S1.

REFERENCES

1. Veit, R.R., Silverman, E.D., and Everson, I. (1993). Aggregation patterns of pelagic predators and their principal prey, Antarctic krill, near South Georgia. J. Anim. Ecol. *62*, 551–564.

2. Benoit-Bird, K.J., Battaile, B.C., Heppell, S.A., Hoover, B., Irons, D., Jones, N., Kuletz, K.J., Nordstrom, C.A., Paredes, R., Suryan, R.M., et al. (2013). Prey patch patterns predict habitat use by top marine predators with diverse foraging strategies. PLoS One *8*, e53348. https://doi.org/10.1371/journal.pone.0053348.

3. Cassini, M.H. (1999). The evolution of reproductive systems in pinnipeds. Behav. Ecol. *10*, 612–616. https://doi.org/10.1093/beheco/10.5.612.

4. Stokes, D.L., and Boersma, P.D. (2000). Nesting density and reproductive success in a colonial seabird, the Magellanic penguin. Ecology *81*, 2878–2891. https://doi.org/10.1890/0012-9658(2000)081[2878:NDARSI]2.0.CO;2.

5. Yen, P.P.W., Sydeman, W.J., and Hyrenbach, K.D. (2004). Marine bird and cetacean associations with bathymetric habitats and shallow-water topographies: implications for trophic transfer and conservation. J. Mar. Syst. *50*, 79–99. https://doi.org/10.1016/j.jmarsys.2003.09.015.

6. Camp, C.L. (1980). Large ichthyosaurs from the Upper Triassic of Nevada. Palaeontogr. Abt. A *170*, 139–200.

7. Hogler, J.A. (1992). Taphonomy and paleoecology of *Shonisaurus popularis* (Reptilia: ichthyosauria). Palaios *7*, 108–117. https://doi.org/10.2307/3514800.

8. Block, B.A., Jonsen, I.D., Jorgensen, S.J., Winship, A.J., Shaffer, S.A., Bograd, S.J., Hazen, E.L., Foley, D.G., Breed, G.A., Harrison, A.L., and Ganong, J.E. (2011). Tracking apex marine predator movements in a dynamic ocean. Nature *475*, 86–90. https://doi.org/10.1038/nature10082.

9. Piatt, J., and Methven, D. (1992). Threshold foraging behavior of baleen whales. Mar. Ecol. Prog. Ser. *84*, 205–210 http://www.jstor.org/stable/24829558.

10. Norris, R.D., Turner, S.K., Hull, P.M., and Ridgwell, A. (2013). Marine ecosystem responses to Cenozoic global change. Science *341*, 492–498. https://doi.org/10.1126/science.1240543.

11. Kidwell, S.M. (2015). Biology in the Anthropocene: challenges and insights from young fossil records. Proc. Natl. Acad. Sci. USA *112*, 4922–4929. https://doi.org/10.1073/pnas.1403660112.

12. Pyenson, N.D., Irmis, R.B., Lipps, J.H., Barnes, L.G., Mitchell, E.D., and McLeod, S.A. (2009). Origin of a widespread marine bonebed deposited during the Middle Miocene Climatic Optimum. Geology *37*, 519–522. https://doi.org/10.1130/G25509A.1.

13. Delsett, L.L., Novis, L.K., Roberts, A.J., Koevoets, M.J., Hammer, Ø., Druckenmiller, P.S., et al. (2016). The Slottsmøya marine reptile lagerstätte: depositional environments, taphonomy and diagenesis. Geol. Soc. Spec. Publ. *434*, 165–188. https://doi.org/10.1144/SP434.2.

14. Balini, M., Jenks, J.F., Martin, R., McRoberts, C.A., Orchard, M.J., and Silberling, N.J. (2015). The Carnian/Norian boundary succession at Berlin-Ichthyosaur State Park (Upper Triassic, central Nevada, USA). Paläontol. Z. *89*, 399–433. https://doi.org/10.1007/s12542-014-0244-2.

15. Martindale, R.C., Corsetti, F.A., James, N.P., and Bottjer, D.J. (2015). Paleogeographic trends in Late Triassic reef ecology from northeastern Panthalassa. Earth Sci. Rev. *142*, 18–37. https://doi.org/10.1016/j.earscirev.2014.12.004.

16. Silberling, N.J. (1959). Pre-Tertiary stratigraphy and Upper Triassic paleontology of the Union District, Shoshone Mountains, Nevada, U.S. Geol. Surv. Prof. Pap. *322*, 1–67.

17. de Buffrénil, V., and Mazin, J. (1990). Bone histology of the ichthyosaurs: comparative data and functional interpretation. Paleobiology *16*, 435–447. http://www.jstor.org/stable/2400968.

18. McGowan, C., and Motani, R. (1999). A reinterpretation of the Upper Triassic ichthyosaur *Shonisaurus*. J. Vertebr. Paleontol. *19*, 42–49. https://doi.org/10.1080/02724634.1999.10011121.

19. Dal Corso, J., Ruffell, A., and Preto, N. (2018). The Carnian Pluvial Episode (Late Triassic): new insights into this important time of global environmental and biological change. J. Geol. Soc. Lond. *175*, 986–988. https://doi.org/10.1144/jgs2018-185.

20. Greene, A.R., Scoates, J.S., Weis, D., Katvala, E.C., Israel, S., and Nixon, G.T. (2010). The architecture of oceanic plateaus revealed by the volcanic stratigraphy of the accreted Wrangellia oceanic plateau. Geosphere *6*, 47–73. https://doi.org/10.1130/GES00212.1.

21. Mazaheri-Johari, M., Gianolla, P., Mather, T.A., Frieling, J., Chu, D., and Dal Corso, J. (2021). Mercury deposition in western Tethys during the Carnian Pluvial Episode (Late Triassic). Sci. Rep. *11*, 17339. https://doi.org/10.1038/s41598-021-96890-8.

22. Dickens, G.R., O'Neil, J.R., Rea, D.K., and Owen, R.M. (1995). Dissociation of oceanic methane hydrate as a cause of the carbon isotope excursion at the end of the Paleocene. Paleoceanography *10*, 965–971. https://doi.org/10.1029/95PA02087.

23. Beardmore, S.R., and Furrer, H. (2016). Evidence of a preservational gradient in the skeletal taphonomy of Ichthyopterygia (Reptilia) from Europe. Palaeogeo. Palaeoclim Palaeoecol. *443*, 131–144. https://doi.org/10.1016/j.palaeo.2015.11.049.

24. Scheyer, T.M., Romano, C., Jenks, J., and Bucher, H. (2014). Early Triassic marine biotic recovery: the predators' perspective. PLoS One *9*, e88987. https://doi.org/10.1371/journal.pone.0088987.

25. Massare, J.A., Lomax, D.R., and Klein, A. (2015). A large forefin of *Ichthyosaurus* from the U.K., and estimates of the size range of the genus. Paludicola *10*, 119–135.

26. Klein, N., Schmitz, L., Wintrich, T., and Sander, P.M. (2020). A new cymbospondylid ichthyosaur (Ichthyosauria) from the Middle Triassic (Anisian) of the Augusta Mountains, Nevada, USA. J. Syst. Palaeontol. *18*, 1167–1191. https://doi.org/10.1080/14772019.2020.1748132.

27. Kosch, B.F. (1990). A revision of the skeletal reconstruction of *Shonisaurus popularis* (Reptilia: ichthyosauria). J. Vertebr. Paleontol. *10*, 512–514. https://doi.org/10.1080/02724634.1990.10011833.

28. Stinnesbeck, W., Frey, E., Rivas, L., Perez, J.P., Cartes, M.L., Soto, C.S., and Lobos, P.Z. (2014). A Lower Cretaceous ichthyosaur graveyard in deep marine slope channel deposits at Torres del Paine National Park, southern Chile. Geol. Soc. Am. Bull. *126*, 1317–1339. https://doi.org/10.1130/B30964.1.

29. Kear, B.P. (2006). Marine reptiles from the Lower Cretaceous of South Australia: elements of a high-latitude cold-water assemblage. Palaeontology *49*, 837–856. https://doi.org/10.1111/j.1475-4983.2006.00569.x.

30. Maxwell, E.E., and Dececchi, T.A. (2013). Ontogenetic and stratigraphic influence on observed phenotypic integration in the limb skeleton of a fossil tetrapod. Paleobiology *39*, 123–134. https://doi.org/10.1666/0094-8373-39.1.123.

31. Massare, J.A. (1987). Tooth morphology and prey preference of Mesozoic marine reptiles. J. Vertebr. Paleontol. *7*, 121–137.

32. Nicholls, E.L., and Manabe, M. (2004). Giant ichthyosaurs of the Triassic—a new species of *Shonisaurus* from the Pardonet Formation (Norian: Late Triassic) of British Columbia. J. Vertebr. Paleontol. *24*, 838–849. https://doi.org/10.1671/0272-4634(2004)024[0838:GIOTTN]2.0.CO;2.

33. Sander, P.M., Chen, X., Cheng, L., and Wang, X. (2011). Short-snouted toothless ichthyosaur from China suggests Late Triassic diversification of suction feeding ichthyosaurs. PLoS One *6*, e19480. https://doi.org/10.1371/journal.pone.0019480.

34. McGaughey, G., Noble, P., Kelley, N., Irmis, R., and dePolo, P. (2021). Hunting for the latest large-bodied ichthyosaur in the Upper Triassic Luning Formation, Mineral County, Nevada, U.S.A. Geol. Soc. Am. Abst. Prog. *53*. 11–11.

35. Stanley, G.D.J. (1979). Paleoecology, structure, and distribution of Triassic coral buildups in western North America. Univ. Kans. Paleontol. Contrib. *68*, 1–58.

36. Callaway, J.M., and Massare, J.A. (1989). *Shastasaurus altispinus* (Ichthyosauria, Shastasauridae) from the Upper Triassic of the El Antimonio district, northwestern Sonora, Mexico. J. Paleontol. *63*, 930–939.

37. McGowan, C., and Motani, R. (2003). Handbook of Paleoherpetology: volume 8, Ichthyopterygia (Verl. Dr. Friedrich Pfeil).

38. Adams, T.L. (2009). Deposition and taphonomy of the Hound Island Late Triassic vertebrate fauna: fossil preservation within subaqueous gravity flows. Palaios *24*, 603–615. https://doi.org/10.2110/palo.2009.p09-010r.

39. Slater, G.J., Goldbogen, J.A., and Pyenson, N.D. (2017). Independent evolution of baleen whale gigantism linked to Plio-Pleistocene ocean dynamics. Proc. Biol. Sci. *284*, 20170546. https://doi.org/10.1098/rspb.2017.0546.

40. Jenks, J.F., Monnet, C., Balini, M., Brayard, A., and Meier, M. (2015). Biostratigraphy of Triassic ammonoids. In Ammonoid Paleobiology: From macroevolution to paleogeography, C. Klug, D. Korn, K. De Baets, I. Kruta, and R.H. Mapes, eds. (Springer), pp. 329–388.

41. Motani, R., Jiang, D.Y., Tintori, A., Rieppel, O., and Chen, G.B. (2014). Terrestrial origin of viviparity in Mesozoic marine reptiles indicated by Early Triassic embryonic fossils. PLoS One *9*, e88640. https://doi.org/10.1371/journal.pone.0088640.

42. Maxwell, E.E., and Caldwell, M.W. (2003). First record of live birth in Cretaceous ichthyosaurs: closing an 80 million year gap. Proc. Biol. Sci. *270*, S104–S107. https://doi.org/10.1098/rsbl.2003.0029.

43. Deeming, D., Halstead, L., Manabe, M., and Unwin, D.M. (1993). An ichthyosaur embryo from the Lower Lias (Jurassic: Hettingan) of Somerset, England, with comments on the reproductive biology of ichthyosaurs. Mod. Geol. *18*, 423–442.

44. Corkeron, P.J., and Connor, R.C. (1999). Why do baleen whales migrate? Mar. Mamm. Sci. *15*, 1228–1245.

45. Clapham, P. (2001). Why do baleen whales migrate? A response to Corkeron and Connor. Mar. Mamm. Sci. *17*, 432–436.

46. Vermeij, G.J. (1977). The Mesozoic marine revolution: evidence from snails, predators and grazers. Paleobiology *3*, 245–258.

47. Knoll, A.H., and Follows, M.J. (2016). A bottom-up perspective on ecosystem change in Mesozoic oceans. Proc. Biol. Sci. *283*. 20161755. https://doi.org/10.1098/rspb.2016.1755.

48. Fröbisch, N.B., Fröbisch, J., Sander, P.M., Schmitz, L., and Rieppel, O. (2013). Macropredatory ichthyosaur from the Middle Triassic and the origin of modern trophic networks. Proc. Natl. Acad. Sci. USA *110*, 1393–1397. https://doi.org/10.1073/pnas.1216750110.

49. Sander, P.M., Griebeler, E.M., Klein, N., Juarbe, J.V., Wintrich, T., Revell, L.J., and Schmitz, L. (2021). Early giant reveals faster evolution of large body size in ichthyosaurs than in cetaceans. Science *374*, eabf5787. https://doi.org/10.1126/science.abf5787.

50. Kelley, N.P., and Pyenson, N.D. (2015). Vertebrate evolution. Evolutionary innovation and ecology in marine tetrapods from the Triassic to the Anthropocene. Science *348*, aaa3716. https://doi.org/10.1126/science.aaa3716.

51. Massare, J.A. (1988). Swimming capabilities of Mesozoic marine reptiles: implications for method of predation. Paleobiology *14*, 187–205.

52. Motani, R., Rothschild, B.M., and Wahl, W. (1999). Large eyeballs in diving ichthyosaurs. Nature *402*, 747.

53. Fischer, V., Arkhangelsky, M.S., Uspensky, G.N., Stenshin, I.M., and Godefroit, P. (2014). A new Lower Cretaceous ichthyosaur from Russia reveals skull shape conservatism within Ophthalmosaurinae. Geol. Mag. *151*, 60–70. https://doi.org/10.1017/S0016756812000994.

54. Oliver, J., Slattery, P., Silberstein, M., and O'Connor, E. (1983). A comparison of gray whale, *Eschrichtius robustus*, feeding in the Bering Sea and Baja California. Fish. Bull. *81*, 513–522.

55. Behar, F., Beaumont, V., and De B. Penteado, H.L. (2001). Rock-Eval 6 technology: performances and developments. Oil Gas Sci. Technol. *56*, 111–134.

56. Geological Society of America (1991). Rock-Color Chart (Geological Society of America).

57. Folk, R.L. (1959). Practical petrographic classification of limestones. Am. Assoc. Petrol. Geol. Bull. *43*, 1–38.

58. Dunham, R.J. (1962). Classification of carbonate rocks according to depositional texture. AAPG Mem. *1*, 108–121.

59. Baccelle, L., and Bosellini, A. (1965). Diagrammi per la stima visiva della composizione percentuale nelle rocce sedimentarie. Annali dell'Università degli di Ferrara, Sezione IX, Scienze Geologiche e Paleontologiche *4*, 59–62.

60. Percival, L.M.E., Ruhl, M., Hesselbo, S.P., Jenkyns, H.C., Mather, T.A., and Whiteside, J.H. (2017). Mercury evidence for pulsed volcanism during the end-Triassic mass extinction. Proc. Natl. Acad. Sci. USA *114*, 7929–7934. https://doi.org/10.1073/pnas.1705378114.

61. Grasby, S.E., Beauchamp, B., Bond, D.P.G., Wignall, P.B., and Sanei, H. (2016). Mercury anomalies associated with three extinction events (Capitanian crisis, latest Permian extinction and the Smithian/Spathian extinction) in NW Pangea. Geol. Mag. *153*, 285–297. https://doi.org/10.1017/S0016756815000436.

STAR★METHODS

KEY RESOURCES TABLE

REAGENT or RESOURCE	SOURCE	IDENTIFIER
Deposited data		
Quarry 2 3D surface model	This Paper	EZID: http://n2t.net/ark:/65665/33ca0e041-4ae9-4b74-bfab-fd9885f2dffa3D.si.edu: https://3d.si.edu/object/3d/25748134-a3ec-4a4a-868b-8192ec73f6a6
microCT scans of *Shonisaurus* embryo/neonate material	This Paper	MorphoSource.org: ark:/87602/m4/476920 ark:/87602/m4/477288

RESOURCE AVAILABILITY

Lead contact
Correspondence and requests for materials should be addressed to Neil Kelley, neil.p.kelley@vanderbilt.edu.

Materials availability
This study did not generate new unique reagents.

Data and code availability
Fossil locality data are not publicly available, but kept on file at UMNH along with geologic samples and thin sections. Fossils included in this manuscript are identified by specimen number and available for study with permission from their home institution (see below).

The μCT datasets generated by the current study are available at Morphosource: https://www.morphosource.org/projects/000476372 and 3D surface data at: https://3d.si.edu/object/3d/25748134-a3ec-4a4a-868b-8192ec73f6a6. The 3D model is also catalogued in the collections of the Smithsonian National Museum of Natural History: http://n2t.net/ark:/65665/33ca0e041-4ae9-4b74-bfab-fd9885f2dffa.

This paper does not report original code.

Any additional information required to reanalyze the data reported in this paper is available from the lead contact upon request.

EXPERIMENTAL MODEL AND SUBJECT DETAILS

Museum abbreviations
BISP – Berlin-Ichthyosaur State Park; NSMLV – Nevada State Museum, Las Vegas; UMNH – Natural History Museum of Utah; UCMP – University of California Museum of Paleontology

Information about the specimens
Fossils in Quarry 2 were digitized but otherwise left undisturbed *in-situ*. Newly collected fossil material is reposited at UMNH under permit agreement with the United States Forest Service. Additional data was acquired from previously collected material reposited at NSMLV, UCMP and BISP as well as from additional published and unpublished sources see details below and in supplemental materials.

METHOD DETAILS

Capturing, processing and rendering 3D digital datasets
We documented *in situ* skeletal remains of *Shonisaurus* in Quarry 2 using three-dimensional digitization techniques. Photogrammetry datasets were captured using a prime 35mm Canon L series lens on a Canon 5D Mark III camera body. Scale was set for the photogrammetry data using scale bars designed by the Bureau of Land Management and produced and calibrated by Cultural Heritage Imaging. We also used a FARO Focus 3D X 330 medium range spherical laser scanner to supplement the photogrammetry data sets and to verify the scale, topography, and alignment of the 3D model derived from the photogrammetry data sets. We used X-Rite ColorChecker targets for color calibration of the photogrammetry image sets and produced color corrected images using the X-Rite ColorChecker software and Adobe Camera Raw. Agisoft PhotoScan 1.2 was used for photogrammetry model creation; Geomagic Studio 2012 for model cleanup and noise reduction along with alignment and comparison of the photogrammetry and laser data; Zbrush v. 4R3 for further model cleanup and noise reduction.

Embryo remains were µCT scanned using the North Star Imaging µCT scanner of the Department of Earth and Environmental Sciences at Vanderbilt University (TN, USA). Voxel size ranged from 20.8 to 32.5 µm, beam voltage ranged from 77 to 121 kV. Volume was reconstructed using EFX-CT (North Star Imaging, Minnesota, USA). Scans were segmented using Object Research Systems application Dragonfly. We used R 4.0.5, Adobe Photoshop and Adobe Illustrator for data analysis and visualization.

Taphonomy and size distribution

Standard measurements (e.g. humerus proximodistal length, vertebra anteroposterior length and average diameter) were measured using measuring tapes or calipers, recorded to the nearest millimeter. Skeleton orientations in Quarry 2 were measured using a Brunton compass to determine the declination of the main body axis of each skeleton. When a skeleton was bent, or partially disarticulated, separate declinations were recorded for each segment. Photographs and 3D models were used to verify and build upon direct observations in the field. Additional data were compiled from published and unpublished sources including Camp[6] and original field notes and drawings archived at UCMP.

The taphonomic state (completeness and articulation, following Mazaheri-Johari et al.[21]) of each specimen within Quarry 2 was assessed directly over the course of multiple visits to the site between 2014 and 2019. Additionally, a high-resolution digital model of the quarry was generated using laser scanning with a Faro Focus 3D and photogrammetry using digital SLR cameras (supplemental materials). This model was used to generate a high-resolution orthographic photomosaic of the quarry (Figures 2 and S1A) which in turn was used to create a detailed quarry map (Figures S1B and S1C). The digital model, orthographic photo and quarry map provided a complementary source of data for scoring the completeness and articulation state of each specimen within the quarry. Finally, these observations were compared with previous assessments.[6,7,18,27]

In addition to scoring the seven specimens preserved *in situ* within Quarry 2, we calculated approximate completeness and articulation scores for eleven additional specimens from six additional localities within the Luning Formation at West Union Canyon (Table S3). Ten of these specimens were specimens reported by Camp in his description of *Shonisaurus*[6] or his field notes, quarry maps and photographs obtained from the archives of the University of California Museum of Paleontology. The published and unpublished descriptions, diagrams and photographs were used to estimate completeness and articulation scores for these specimens (Figure S2). Five of these specimens are in collections at the Nevada State Museum, Las Vegas and one specimen is still visible in the park although it is exposed to the environment and its condition has likely deteriorated since its initial discovery. The current status of the other five specimens is unknown and they may have been lost or reburied. One additional new specimen (UMNH VP 32545) discovered during the course of our investigations in 2015 was excavated and collected in 2016–2017. Although this specimen awaits complete preparation and study, its articulation and completeness were scored from photographs, field notes and quarry maps and included in this analysis.

Field investigation and geological methods

In addition to examination of *in situ* fossils in Quarry 2, we relocated three additional quarries (3, 5 and 6) and determined the approximate location of other original localities. We systematically searched all three members of the Luning Formation exposed in WUC for additional vertebrate fossils and recorded their location with handheld GPS receivers. We used existing geologic maps and stratigraphic sections as well as associated invertebrate fossils to determine the stratigraphic positions of these localities.

In the field, hand tools were used to expose (between ~30-150 cm below the surface) a continuous vertical profile of fresh, unweathered strata at quarries 2, 5, and 6. The strike and dip of beds was measured using a Brunton Pocket Transit, and these values used to correct stratigraphic unit thickness measurements taken with a Precision Jacob's Staff (ASC Scientific). Each unit was described in fresh hand sample and characterized using a Munsell Rock Color Chart.[56] Carbonate layers were also described in thin section using a binocular petrographic microscope in both plane and cross-polarized light. Carbonate classification follows Folk[57] and Dunham,[58] and the densities of clasts and fossils were estimated using charts from Baccelle and Bosellini.[59] Unweathered samples were collected at 10–50 cm intervals from every unit for geochemical analysis.

Fresh surfaces on each sample were cleaned with deionized water, air-dried, and then powdered using a shatter box. To acidify the samples prior to analysis of total organic carbon content (TOC) and bulk $\delta^{13}C_{org}$ values, 10-15 ml was placed in a clean 100 ml beaker to which 60 ml of 1M HCl was added. Theses beakers were then placed in a 50°C water bath for 24 hours, after which the samples were filtered with deionized water using a vacuum pump and oven dried. Approximately 25 mg of each sample was weighed for $\delta^{13}C_{org}$ and TOC measurements made using a Thermo Finnigan Delta Plus XL IRMS connected to a Carlo Erba Elemental Analyzer (EA, model 1010) via a Thermo Finnigan Conflo III at the Stable Isotope Ratio Facility for Environmental Research (SIRFER), University of Utah. These analyses did not use He dilution, and raw data were normalized using three sets of internal lab reference materials (PLRM-1, PLRM-2, and SLRM) that are calibrated against USGS40 and USGS41.

A subset of untreated bulk powdered samples was also analyzed to determine TOC without acidification and characterize kerogen type and maturity, using a Rock-Eval VI at the University of Oxford.[55] TOC values were very low for all measured samples, with only one sample exceeding 0.2 wt%, with the low quantity of kerogen hindering robust interpretation of the other measured Rock-Eval parameters. The mercury concentrations of untreated bulk powdered samples were determined on a RA-915 Portable Mercury Analyzer with PYRO-915 Pyrolyzer (Lumex) at the University of Oxford, following the procedure outlined in Percival et al.[60] Two aliquots of 50 ± 2 mg were measured to check reproducibility, which was better than ±10%, with NIST/UOE/FM/001 – Inorganic Elements in Peat (169 ppb Hg) utilized as a reference material to ensure machine accuracy. Hg concentrations show considerable variations throughout the stratigraphy at Quarry 2, ranging 2.6 to 139.5 ppb. The lithology is not suggestive of a strongly

oxygen-depleted environment, nor do the Hg peaks show a clear correlation with lithological variations, suggesting that deposited mercury was not influenced by redox or lithology changes, and was primarily deposited with organic matter. However, interpretation of the Hg/TOC values is hindered by most samples featuring a TOC content below that recommended for mercury normalization.[61] Geochemical data are shown on Figures 1 and S3 and reported in Table S2.

QUANTIFICATION AND STATISTICAL ANALYSIS

Quantitative data presented in Figures 1, 3, and S3 and Tables 1 and S1–S3 were compiled and calculated in Microsoft Excel and R version 4.0.3. following the methods detailed above.